Laser-induced electric breakdown in water

C. A. Sacchi

Centro di Elettronica Quantistica e Strumentazione Elettronica del Consiglio Nazionale delle Ricerche, Istituto di Fisica del Politecnico, piazza Leonardo da Vinci 32, 20133 Milano, Italy

Received March 1990; accepted June 19, 1990

Dielectric breakdown induced in water by Nd:YAG laser pulses is considered experimentally and theoretically. The effect appears to be due to electron avalanche ionization. The aspects of this process considered here are the following: (i) The dependence of the breakdown probability on the laser field. At high fields, electron interaction with molecular (Raman) vibrations or with collective molecular motions occurs. (ii) Bragg scattering, which contributes to keeping the electron motion in phase with the optical field. (iii) The role of the electron mobility, which contributes to stabilizing the process. (iv) The generation of the electrons that start the avalanche in relation to different laser-pulse durations and irradiances.

INTRODUCTION

Laser-induced electric breakdown in transparent dielectrics has been studied extensively. The importance of this effect for the production of a laser-induced plasma and for the propagation of high-irradiance laser beams through matter was quickly recognized: it is of relevance, for example, for the study of damage of laser materials and optical components in large systems used for the generation of high-power laser pulses. Since it is produced by a beam with high irradiance, this effect is complicated because several nonlinear-optical effects can occur. Experimental investigations have been performed mainly for gases and in solids: several reviews have been published.[1-4] For liquids the investigation has been devoted mainly to the analysis of sparks and shock waves.[5,6]

The occurrence of electric breakdown in liquids, as produced by short laser pulses with high irradiance, has become of interest in the past few years in connection with medical applications of lasers such as for ophthalmic microsurgery[7-9] and, more recently, stone fragmentation.[10] In the former case, laser pulses generated by a Q-switched or, less frequently, mode-locked Nd:YAG laser are focused inside the vitreous of the eye to disrupt vitreal strands or membranes or, more commonly, on the posterior wall of the capsule in the presence of a secondary cataract. Mechanical disruption is due to a shock wave generated in the expansion of the absorbing plasma created by the focused laser pulses. Absorption by the plasma also partially shields the fundus of the eye from the incoming laser energy. Studies performed *in vitro,* on eye models, and *in vivo* have shown that breakdown under laser irradiation is a probabilistic event and that the degree of probability is related to the beam irradiance. The aim of these studies was to find the minimum value of beam irradiance that ensures 100% probability of breakdown. The interpretation of the basic effects, however, has been referred to the existing literature on breakdown in gases and solids.[11]

Laser-induced breakdown in the liquids of interest for the ophthalmic applications has been studied by measuring the probability of its occurrence at different values of the laser irradiance. This has been done by changing the laser power, the focusing optics, and the pulse duration.[12,13] It has been found, in particular, that the breakdown probability has a dependence on the laser field similar to that found in solids.[14] Furthermore, also in this case, the threshold obtained with optical fields is of the same order of magnitude as that obtained with dc fields. These data suggest that the main mechanism responsible for the occurrence of breakdown in liquids is electron avalanche ionization, as in solids.

Here I report on new experimental results and discuss some basic physical aspects of the electric breakdown induced in water samples with different degrees of purity by laser pulses generated by a Nd:YAG laser. In order to clarify the experimental results, the following aspects are considered: (i) The dependence of the logarithm of the breakdown probability on the reciprocal laser field. This dependence is linear at low fields and parabolic at high fields, where electron scattering by optical phonons occurs. (ii) The mechanism that keeps the electrons in phase with the optical field, allowing them to gain energy. (iii) The importance of the electron mobility in dense water vapor, which has a stabilizing role in the process. (iv) The generation of the initial electrons that start the avalanche, in relation to the laser-pulse irradiance and duration.

EXPERIMENTAL APPARATUS

The experimental apparatus has already been described in detail.[12,13] Two Nd:YAG laser sources, operating at 1.064 μm, were used: (i) A passively Q-switched laser, which generated pulses with smooth temporal and spatial profiles. The pulse duration (FWHM) was 7 or 12 nsec in two different configurations. The spatial configuration was TEM_{00} mode with 10-mJ energy or multimode with energy as high as 200 mJ. The pulse energy, varied through a series of calibrated attenuators placed in the beam path, was measured by a pyroelectric detector. The beam divergence was 4.5 mrad in the multimode configuration and 1.2 mrad in the TEM_{00} mode. (ii) An actively–passively mode-locked laser system (Quantel Model 402),

0740-3224/91/020337-09$05.00

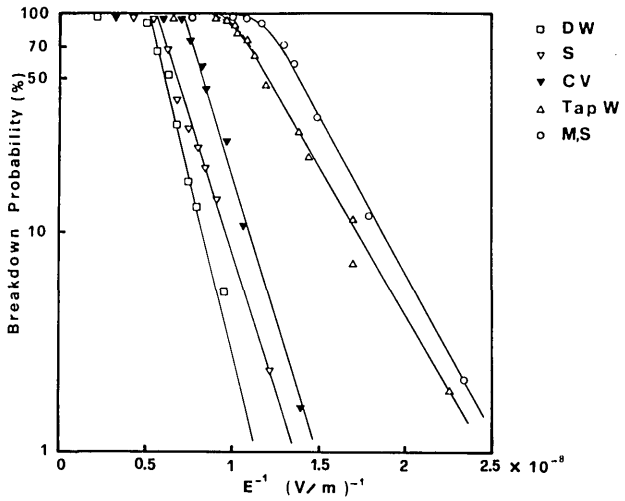

Fig. 1. Breakdown curves expressed as the logarithm of breakdown probability versus the inverse of the laser electric field. The spot size (1/e of the peak irradiance) was $d = 350$ μm; the pulse duration was $t_L = 7$ nsec. DW, distilled water; S, saline solution; CV, calf vitreous; Tap W, tap water; M,S, thin (10-μm) plastic membrane in saline solution.

which generated single pulses with a TEM_{00} mode. The pulse duration could be switched between 220 and 30 psec by changing the resonator length and the driving frequency of the acousto-optic modulator. Pulse energies as great as 25 mJ with 220-psec pulses and 5 mJ with 30-psec pulses were used. The energy, changed by varying the supply voltage of the flash lamps in the two system amplifiers, was measured with a calorimeter. The beam divergence was 0.56 mrad. The irradiance, in the focal plane of quartz lenses, was calculated by dividing the pulse energy by the pulse duration and by the area of the focal spot. The spot diameter was taken at 1/e of the peak value. This calculation could be affected by nonlinear-optical effects, whose occurrence was investigated with nanosecond pulses. Self-focusing and stimulated Raman scattering were not observed in these experimental conditions. A backscattered beam, attributed to the stimulated Brillouin effect, was indeed observed with a threshold of 5 GW/cm^2, but the associated energy was only a few percent of the input energy.

The liquids used were (1) double-distilled water (Baxter, S.p.A., Trieste, Italy), (2) 0.9% saline solution (Baxter, S.p.A., Trieste, Italy), (3) tap water, (4) high-pressure liquid chromatography (HPLC) water (Aldrich Chemical Company, Milwaukee). For biomedical purposes fresh calf vitreous was also tested. Breakdown curves were obtained[12,13] by plotting, for each value of the laser irradiance, the probability of occurrence of breakdown, monitored either visually or by a photomultiplier. At least 30 pulses were considered at each irradiance. The pulse repetition rate was 1 Hz.

RESULTS

Typical behavior of the breakdown probability, on a logarithmic scale, versus the reciprocal laser field is represented in Figs. 1 and 2 for all the liquids examined. This representation was chosen for comparison with the data obtained for both crystalline and amorphous solids.[14] For each figure the focusing optics, and therefore the beam spot size, was fixed. When the focusing optics for a given material is changed, the data change. Indeed, the threshold irradiance (defined as the minimum irradiance that gives 100% breakdown probability) increases with the reciprocal spot size of the focused beam, i.e., with the divergence of the input beam and with the power of the focusing lens. Examples of this behavior have been published.[12,13]

The same kinds of measurement were done in distilled water with single laser pulses of different durations: 7 nsec and 220 and 30 psec. The results are shown in Fig. 3. Finally, the behavior of the threshold irradiance for different pulse durations in different samples is shown in Fig. 4. Measurements in HPLC water were performed in a nitrogen atmosphere.

DISCUSSION

The data shown in Fig. 1 are similar to those of solids.[14] As in this case, the breakdown probability P depends on the rms laser field, $\bar{E}$, through the simple relation $P \propto \exp(-K/\bar{E})$ for values of P ranging from a few percent to more than 70%. This dependence has been considered[14] suggestive for an avalanche-breakdown mechanism because the dc ionization coefficient that governs avalanche breakdown in gases and semiconductors depends on the electric field in the same manner. The physical interpretation[14] is the same as that given by Shockley for semiconductors[15] and known as the lucky-electron model. Shockley observed impact ionization produced by electrons that happened to avoid collision. Here the lucky electrons are those that undergo favorable elastic collisions that reverse their momentum when the field reverses, in order to gain energy from the alternating field. The probabilistic nature of the effect relies, then, on the probability of a single electron's being accelerated to the ionizing energy ε_i, and, if the secondary electrons produced by an ionizing collision have a mean energy much greater than KT, the avalanche statistics should be gov-

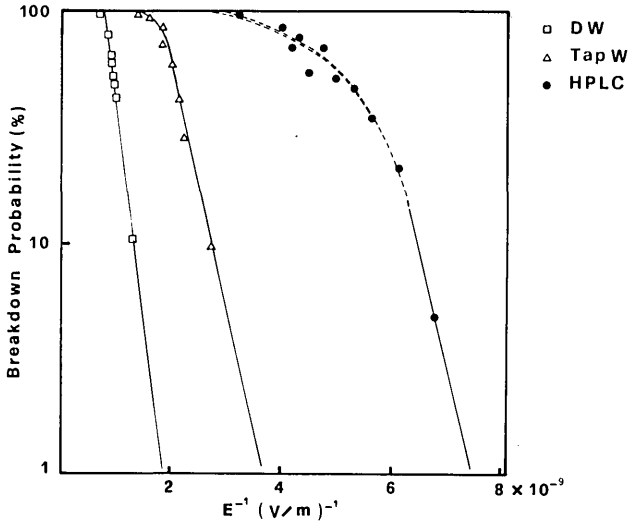

Fig. 2. Breakdown curves, expressed as the logarithm of breakdown probability versus the inverse of the laser electric field. The spot size (1/e of the peak irradiance) was $d = 15$ μm; the pulse duration was $t_L = 12$ nsec. DW, distilled water; Tap W, tap water.

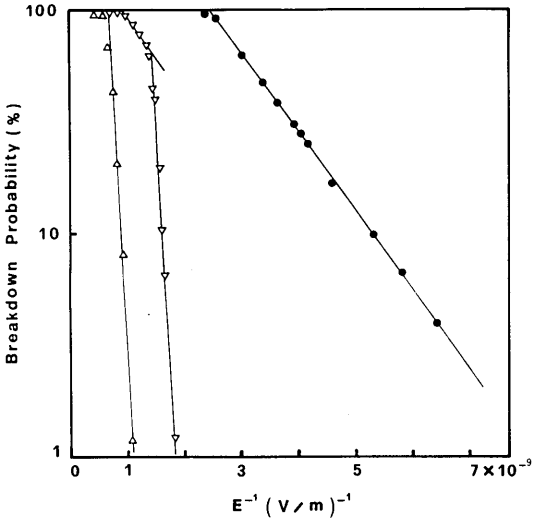

Fig. 3. Breakdown curves, expressed as the logarithm of breakdown probability versus the inverse of the laser electric field, for distilled water and different pulse durations. The spot size ($1/e$ of the peak iraradiance) was $d = 50$ μm. Pulse duration: △, 30 psec; ▽, 220 psec; •, 7 nsec.

erned by the first stage of the avalanche itself. Another important experimental observation, obtained with alkali-halide crystals,[16] is that the rms field strength for laser breakdown is of the same order as the dc breakdown strength. This is intuitively clear[4] if the collision time is so short as to permit a few lucky collisions in one or a few light cycles. The model presented[14] is admittedly highly simplified but gives good agreement with the experimental results. In his review,[4] Bloembergen concludes that laser-induced electron avalanche ionization is usually the mechanism that determines the breakdown threshold in pure transparent crystalline or amorphous solids and liquids. This general conclusion is supported by the results presented here (Fig. 1 and Tables 1 and 2), similar to those for solids.[14] Furthermore, for water the rms field strength is of the same order of magnitude as that at frequencies of a few megahertz.[17] A deeper analysis of the model, to interpret the experiments, appears worthwhile and is presented below.

Models of Electron Multiplication in Solids with a Static Field

The Shockley model[15] describes secondary ionization in semiconductors, given by a dc field, in a phenomenological way. It contains fitting parameters that represent, in an average and equivalent way, complex physical processes. The main point is to consider impact ionization as produced by electrons that happen to avoid collision, in a sort of lucky flight (or lucky ballistic motion). An earlier theory, presented by Wolff,[18] based on the contribution of thermalized electrons with a spherical symmetric distribution (rather than peaked in the forward direction as assumed by Shockley), yields an ionization coefficient with a different dependence on the electric field [$\exp(-K'/\bar{E}^2)$ rather than $\exp(-K/\bar{E})$]. A more refined theory was presented by Baraff,[19] who calculated the ionization coefficient by first computing the hot-electron distribution numerically from the Boltzmann equation at low temperature. His results, which have been widely applied to experiments, give a dependence of the ionization coefficient on the field strength of roughly $\exp(-K/\bar{E})$ at low fields and $\exp(-K'/\bar{E}^2)$ at high fields but with significant differences from the earlier calculations of Wolff and Shockley. Similar results were obtained by Keldysh,[20] who solved the problem of impact ionization in semiconductors in analytic form and for arbitrary values of the field E and of the temperature T. Then Ridley[21] used a new approach to the problem based on the difference between momentum- and energy-relaxation rates for hot electrons. The basic mechanism whereby an electron gains sufficient energy to ionize is a lucky drift (rather than a ballistic motion) in which the electrons relax momentum but not energy. According to this model neither the Shockley lucky electron nor the Wolff thermalized electron contributes significantly, in agreement with Baraff. The theory has a wide application to semiconductors with moderate to large energy gaps because of the predominance of nonpolar scattering at high energies, but a mean free path is taken as an average quantity over the relevant energy range. Finally the model shows why the Wolff-like mechanism [$P \propto \exp(-K'/\bar{E}^2)$] dominates at high fields and the Shockley-like mechanism [$P \propto \exp(-K/\bar{E})$] dominates at low fields. Much earlier, Seitz[22] investigated the theory of the multiplication of electrons in strong electric fields in crystals. After reviewing previous theories Seitz faced the problem of investigating whether breakdown and related properties are determined by the average electron or by improbable statistical fluctuations in which the electron makes no collisions, thus anticipating the concepts described later by Wolff and Shockley, respectively. Seitz derived an expression for the breakdown probability of the type $\propto \exp(-K/\bar{E})$ for the case of fluctuations and gave the basis for an expression $\propto \exp(-K'/\bar{E}^2)$ for the average electron. He also gave a semiquantitative argument to evaluate, in practice, which behavior would be favored.

Seitz's treatment is now briefly considered, to clarify the meaning of a formalism useful in interpreting the experimental results presented in this paper. An electron

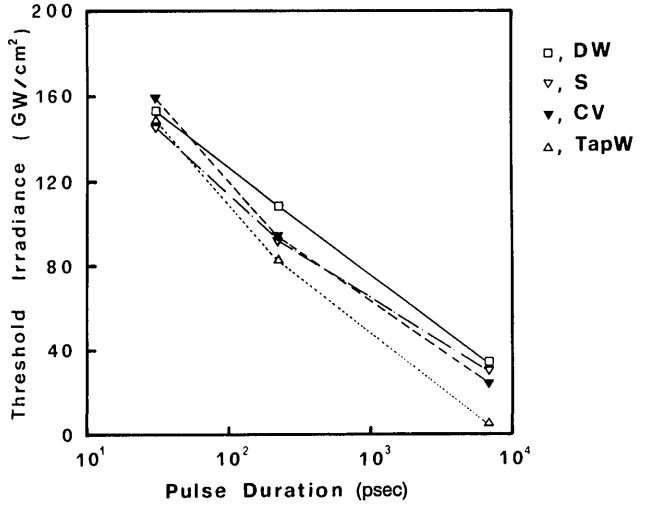

Fig. 4. Breakdown threshold irradiance versus the laser-pulse duration for several media. The spot size ($1/e$ of the peak irradiance) was $d = 75$ μm. DW, distilled water; S, saline solution; CV, calf vitreous; Tap W, tap water.

Table 1. Evaluation of Some Physical Parameters Considered in the Text for the Materials Listed[a]

Material	$\bar{E}_{th}$ (V/m)	K (V/m)	l (Å)	M	α_{100}	α_{50}
Distilled water	1.91×10^8	7.5×10^8	87	25	7.85	9.25
Saline solution	1.76×10^8	5.6×10^8	116	27	6.15	7.7
Tap water	1.00×10^8 (linear region)	3.1×10^8	210	48	6.20	7.7
	1.09×10^8 (parabolic region)					
Calf vitreous	1.38×10^8	5.86×10^8	111	34	8.35	9.8
Membrane in saline solution	0.84×10^8 (linear region)	3.3×10^8	196	57	7.85	9.1
	1.00×10^8 (parabolic region)					

[a]Laser parameters: pulse duration 7 nsec, spot size $d = 350$ μm. Tables 1 and 2 refer to two different irradiation cases. The spot size d has been measured at $1/e$ of the peak irradiance, and the laser pulse duration is the FWHM. $\bar{E}_{th}$ is the rms field at the center of the focal spot. K is the slope of the linear region of Fig. 1. l (Å) has been calculated from $K = \varepsilon_i/ql$, assuming that $\varepsilon_i = 6.5$ eV. M is the number of half-cycles of the field required for the electron to reach ε_i: it is calculated from the duration of the ballistic flight (see text). $\alpha = (2K/\bar{E})$ gives the ratio of probabilities of the ballistic flight and lucky drift. The subscripts 100 and 50 refer to 100% and 50% breakdown probability, respectively.

Table 2. Evaluation of Some Physical Parameters Considered in the Text for the Materials Listed[a]

Material	$\bar{E}_{th}$ (V/m)	K (V/m)	l (Å)	M	α_{100}	α_{50}
Distilled water	1.33×10^9	4.06×10^9	16	3.6	6.1	7
Tap water	0.54×10^9 (linear region)	2.47×10^9	26.3	8	9	9.9
	0.715×10^9 (parabolic region)					
HPLC water	0.182×10^9 (linear region)	2.25×10^9	29	26.4	24.5	25.3
	0.33×10^9 (parabolic region)					

[a]Laser parameters: pulse duration 12 nsec, spot size $d = 15$ μm. The parameters are the same as for Table 1 except that K is the slope of the linear region of Fig. 2.

(charge e, mass m), which moves in the direction of the force exerted by the field E, would be accelerated at the rate eE/m. Hence it would gain energy from the field at the rate

$$d\varepsilon/dt = eEv = eE(2\varepsilon/m)^{1/2}.$$

The probability $P_1(t)$ that it will move for a time t, avoiding a momentum-relaxing collision, satisfies the equation $(dP_1/dt) = -pP_1$, where $p = \tau_m^{-1}$ is the reciprocal of the momentum-relaxation time constant. Since p is a function of energy, which in turn is a function of time, p may be regarded as a function of time. Hence

$$P_1(t) = \exp\left(-\int_0^t p\,dt\right) = \exp\left(-\int_{\varepsilon_1}^{\varepsilon_2} \frac{p\,d\varepsilon}{d\varepsilon/dt}\right), \quad (1)$$

where ε_1 and ε_2 are the initial and final electron energy, respectively. Assuming that $p \propto \varepsilon$, as suggested by Fig. 2a of Ref. 22 [up to an energy ε_z, which is an average of the maximum and minimum energies associated with the boundaries of the first (conduction) Brillouin zone in the crystal], we obtain, after simple substitution

$$P_1 = \exp\left[-\frac{2}{3}\frac{\varepsilon_2 p(\varepsilon_2)}{eEv(\varepsilon_2)}\right], \quad (2)$$

with the assumption that $\varepsilon_1^{1/2}p_1 \ll \varepsilon_2^{1/2}p_2$. If we assume that E and v oscillate in phase at optical frequency and consider the rms field $\bar{E}$, Eq. (1) becomes, for $\varepsilon_2 = \varepsilon_i$ (ionization energy),

$$P_1 = \exp\left(-\psi\frac{\varepsilon_i}{e\bar{E}l_2}\right), \quad (3)$$

with $\psi = 0.94$, $l_2 = v(\varepsilon_i)\tau_{m_2}$, and $\tau_{m_2} = 1/p(\varepsilon_i)$. Equation (3) coincides with the Shockley expression for P if we neglect the factor ψ or if we define a new distance, $l' = l_2/\psi$. Let us consider, on the other hand, an average electron, which undergoes Brownian motion and possesses a mobility $\mu = (e/m)\tau_m$. The electron gains energy from the field at a rate

$$d\varepsilon/dt = (e^2/m)E^2\tau_m.$$

Following Ridley,[21] if τ_ε is the energy-relaxation time constant, the probability of an electron's drifting for a time t and avoiding energy relaxation is

$$P_2 = \exp\left(-\int_0^t \frac{dt}{\tau_\varepsilon}\right) = \exp\left(-\int_0^{\varepsilon_i} \frac{m\,d\varepsilon}{e^2E^2\tau_m\tau_\varepsilon}\right). \quad (4)$$

For interaction with phonons of energy $\hbar\omega$, we can write[21] $\tau_\varepsilon/\tau_m = \varepsilon/\hbar\omega$. Then, assuming, as in the previous case, that $\tau_m^{-1} = p \propto \varepsilon$ and $\varepsilon_i = (1/2)mv_{\varepsilon_i}^2$, we obtain from Eq. (4)

$$P_2 = \exp\left(-\frac{\varepsilon_i}{e\bar{E}l_2}\frac{\hbar\omega}{e\bar{E}l_2}\right), \quad (5)$$

where $l_2 = v_{\varepsilon_i}\tau_{m_2}$, as in Eq. (3), and $\bar{E}$ is the rms field. Equation (5) coincides with the expression for P at high fields given by Keldysh.[20]

The relative importance of the two regimes [ballistic flight, which leads to Eq. (3), and lucky drift, which leads to Eq. (5)] has been evaluated by Seitz[22] for the following somewhat idealized situation. He assumes that the collision frequency p is independent of energy (a fair approximation in ionic crystals) and that the electron loses all its forward momentum, on the average, each time it makes a collision with the crystal lattice and starts at rest. The time interval between collisions, $\bar{t}$, is assumed sufficiently long and the applied field sufficiently strong that the colli-

sions can be regarded as elastic. If the time required for the electron to reach the ionization energy, ε_i, is t_1 through the ballistic flight and $n\bar{t}$ through the lucky drift, the result is

$$n\bar{t} = n^{1/2}t_1 .$$

Seitz then calculates (using a Poissonian distribution) the probability, A, that the electron will undergo n collisions in the time $n^{1/2}t_1$ and the probability, B, that the electron will spend a time t_1 without making a collision in the time interval $n^{1/2}t_1$. The comparison between A and B shows that, for $\alpha = pt_1 \geqq 10$, B is larger than A; i.e., the fluctuations that provide the ballistic flight become dominant (in this case $n^{1/2} = 0.3\alpha$).

When the experimental results obtained in water are analyzed, it is immediately clear that the behavior expressed by both Eqs. (3) and (5) is present but that the former behavior is dominant. Some general aspects should now be considered.

Mechanism of Lucky Collisions with an Optical Field

When breakdown is produced by an optical field, the ballistic flight without collisions must be replaced by a flight in which lucky collisions reverse the electron momentum when the field reverses.[14] We may wonder whether some particular effect is responsible for this kind of collision. As Seitz recognized,[22] an electron, in the course of being accelerated, may pass near the boundary of a Brillouin zone where it has a finite chance of undergoing Laue scattering. Such scattering will alter not the energy of the electron but rather its direction of motion and hence the rate at which it gains energy. In liquid water or in dense vapor, in the presence of large molecular groups, electron backscattering can occur when the electron wavelength, λ_e, satisfies the Bragg condition

$$n\lambda_e = 2d ,$$

where d is the intermolecular distance and n is an integer. The value of λ_e that satisfies the Bragg condition in liquid water at room temperature can be deduced from several scattering experiments. The scattering parameters that yield the maximum in the angular (here at $\theta = \pi$) distribution of neutron scattering[23] give (for $n = 1$) $\lambda_e = 6.28$ Å. On the other hand, from x-ray scattering measurements,[24] a molecular structure function for liquid water is obtained that presents two maxima, at room temperature, at scattering parameter values of 2 and 3, respectively. These maxima merge into a single maximum at increasing temperature. At 200°C this maximum corresponds to a scattering parameter value of 2.44. The corresponding values of λ_e are 4.2 and 6.28 Å (at 20°C) and 5.2 Å (at 200°C). The molecular correlation function, in turn, peaks at $d =$ 2.8–2.9 Å from 4 to 200°C. Similarly, electron scattering measurements[25,26] in liquid water at 5°C give a peak of scattering efficiency at $\lambda_e = 5.7$–6.3 Å. These values of λ_e correspond to electrons with energy of ~3.6–4.3 eV. In all these experiments the scattering intensity distribution and the molecular structure function present broad peaks: their widths correspond to electron energies in the interval 2–8 eV. If we assume an ionization energy $\varepsilon_i = 6.5$ eV (Refs. 27 and 28) for water, the electrons can benefit from Bragg reflection to get the required lucky collisions for most of their energy range. Of course the reflection efficiency increases with the number of cells in the molecular group, and this increase requires the presence of large groups in the medium, making the reflectivity bandwidth narrower. The use of a linearly polarized excitation beam can then induce an anisotropy in the **K** space of the generated electrons, as has been observed in semiconductors. A large fraction of the electrons would hence already possess the direction of motion favorable for gaining energy from the field at the time that the electrons are generated.[29]

Fitting the Experimental Curves of ln P versus $1/\bar{E}$

The breakdown-probability curves represented in Figs. 1 and 2 are similar to those obtained in solids.[14] From these curves the values of the threshold field (which corresponds to 100% breakdown probability) can be obtained. Fitting the linear regions to Eq. (3) also gives values of the slope K and of the characteristic distance l (see Tables 1 and 2) similar to those of solids.[14] As has already been mentioned, an ionization energy $\varepsilon_i = 6.5$ eV has been assumed for liquid water. From the duration $t_1 = (2m\varepsilon_i)^{1/2}/q\bar{E}$ of ballistic flight, the number M of half-cycles of the field required for the electron energy to reach ε_i can also be evaluated.

In solids (alkali halides) the threshold at optical fields ($\lambda = 10.6$ μm) is only slightly higher than with dc fields.[16] The latter threshold is, however, somewhat sensitive to the experimental technique used to measure it. A similar situation is found in water. In fact, the breakdown field in deionized distilled water, with pulses of 2–10 μsec duration, is (2–5) $\times 10^7$ V/m but exhibits a large fluctuation.[17] This value is lower by a factor of 4–9 than the value given in Table 1 for distilled water. These data, in solids, strongly suggest that the breakdown mechanism with optical fields is the same as for dc (or low-frequency) fields.[16]

Also, the parameter $\alpha = pt_1 = (2K/\bar{E})$, introduced by Seitz[22] to evaluate the relative importance of electron fluctuations, has been calculated (Tables 1 and 2) to determine its importance in the present experimental situation. To stay in the region of validity of Eq. (3), I have evaluated $\bar{E}$ for 50% breakdown probability. The values of α should be, in this case, $\geqq 10$. In spite of the semiquantitative character of the criterion, the experimental situation is reasonably well described by the value of α. In fact, when α is evaluated for the linear part of the experimental curves of Figs. 1 and 2, it is ~10 in most of the cases. When taken at higher probability values (e.g., extrapolating the linear part of the curves at $P = 100\%$), α is obviously lower.

Some deviation from the linear part, near $P = 100\%$, occurs in almost all the curves. It is interesting that a parabolic part appears more clearly when α has the lowest values, i.e., in tap water and saline solution. Fitting Eq. (5) to the parabolic part of the experimental curves, with $K = \varepsilon_i/el$ being evaluated from the linear part, yields the phonon energy $\hbar\omega$. This, done for the pronounced case of tap water (Fig. 1), gives $\hbar\omega = 0.45 \pm 0.05$ eV, which corresponds to the Raman vibration of the water molecule $\hbar\omega = 0.40$–0.43 eV. This means that Raman scattering is

induced by the intense laser pulse, even in its initial stage, at least in the spontaneous regime. No stimulated Raman–Stokes scattering has been observed, however, in the present experiment. HPLC water behaves in a different way. Not only is E_{th} lower than for the other, less pure, samples, as discussed below, but also the entire experimental curve appears different from the others. The linear region is limited, at least in the experimental conditions discussed, to values of $P \lesssim 15\%$, and the parabolic arc is highly pronounced: it appears at values of the electric field more than three times lower than for tap water (Fig. 2), where, in the same experimental conditions, the Raman vibrations are excited. Fitting the parabolic curve yields a value of $\hbar\omega = 0.079 \pm 0.01$ eV, which corresponds to the frequency of the collective mode considered, for water, by Ascarelli[30] ($\hbar\omega = 0.078$ eV, i.e., 630 cm^{-1}), which is equivalent to a longitudinal optical phonon. This behavior is exhibited only by ultrapure water, which is likely to possess a more extended local order than the other water samples. The appearance of this phonon scattering at relatively low fields is likely to be responsible for the anomalous value of the α parameter for HPLC water reported in Tables 1 and 2 and for the low threshold of this sample, as discussed below.

Early Stage of Plasma Formation: The Importance of Electron Mobility

The fact that the experimental data are well described by Eq. (3) for most of the samples deserves a further comment. It means that the material has the same value of l, and therefore of τ_m (v is obviously the same, since it refers to the end of the ballistic motion), in a large interval of $\bar{E}$, which may change by as much as a factor of 2. This means a variation by as much as a factor of 4 in the energy density deposited in the focal volume and a consequent different increase of temperature and expansion in the initial transient stage of the process. The importance of the initial stage is verified by many experiments. Time-resolved studies of Nd:YAG-laser-induced breakdown[31] show that there is a plasma luminescence at the beginning of the laser pulse. As for the acoustic transient, the extrapolation to the breakdown time of the distance (versus time) traveled by the transient[31] shows that the transient already exists at that time. Of course, the early presence of luminescence and of the acoustic transient means that the plasma began to be created, to absorb, and to expand before the breakdown time, at the beginning of the laser pulse, in a prebreakdown stage that evolves, presumably, on a subnanosecond time scale. In solids, measurable currents for fields somewhat lower than that required to produce breakdown have in fact been reported.[22] These currents are related to breakdown and suggest that electron avalanches are already present at this stage.

An experimental study of the electron mobility in dense polar vapors[32] is useful in explaining how the effects that occur at the prebreakdown stage can influence the subsequent breakdown. The electron mobility has been studied in supercritical NH_3 vapors and subcritical H_2O vapors as a function of vapor density and temperature. The most comprehensive data have been obtained for supercritical NH_3 vapors, but similar behavior is expected to hold for supercritical H_2O vapor.[32] A schematic drawing of the results is shown represented in Fig. 5, adapted from Fig. 1 of Ref. 32, for the sake of simplicity in the following explanation. Recall that the initial part of the curve (μ proportional to $1/n$) represents quasi-free or extended electron states characterized by large mobilities ($\geqq 10$ cm^2/V sec in water for $n < 10^{20}$ cm^{-3}), while the remaining part represents localized electron states with small mobilities (as little as 10^{-3} cm^2/V sec in water). A minimum is presented at $\sim n_c/2$ (n_c is the critical density), and a maximum at $\sim 2n_c$. The mobility in the liquid and its increase at high temperature are also represented: the lower curve corresponds to a lower temperature. Electron localization is expected to occur in dense orientational clusters, the dimensions of which can increase with n to $\sim n_c/2$, thus decreasing the mobility. In the range $n_c/2 < n < 2n_c$, the increase of mobility is caused by a transition from electrons localized in dense clusters to electrons localized in cavities (solvated electrons). Experimental data at higher vapor density are not available for both NH_3 and water. Let us suppose now that in the laser-irradiated region of the liquid, e.g., in the center, a process, based on electron acceleration by the field and described by Eq. (3), starts. If some radiation absorption produces a temperature increase, according to Fig. 5 the electron mobility μ will increase, and so will l, which is proportional to μ. This will increase the probability P of the process or, for $P = 100\%$, will decrease the value of the threshold field. The process will thus be enhanced, more energy will be delivered to the sample, and vapor will be formed. If the curve μ–n follows the dotted curve between n_{liq} and $2n_c$, vapor expansion with density decrease will produce a further increase of μ. The process will continue until the maximum M is reached. Beyond M the

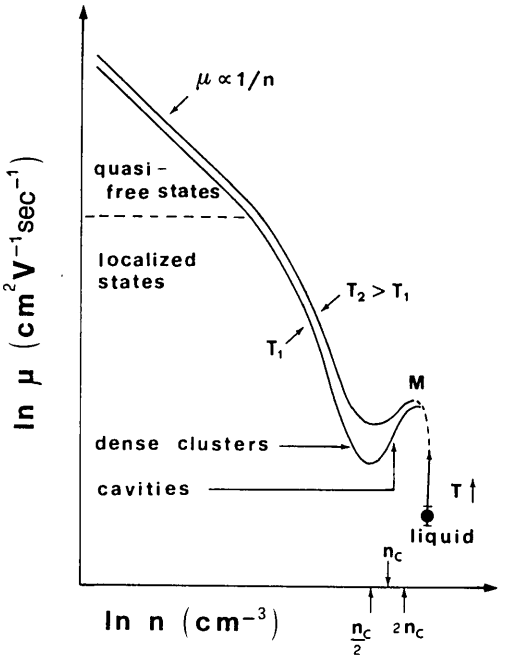

Fig. 5. Electron drift mobility μ in dense NH_3 vapor versus number density n of the vapor for two temperatures (T_1, T_2). This drawing is derived from the data of Krebs (Ref. 32, Fig. 1). Similar behavior is believed to hold for water vapor. n_c, critical density.

process will go in the opposite way: a further decrease of density will produce an increase of the threshold. The process can continue for a while if it starts during the rise time of the laser pulse, but eventually it will return to M. The presence of the maximum, therefore, stabilizes the process. The same mechanism can also produce some spatial confinement: in fact, around the region of expansion some compression will occur. The consequent density increase will raise, locally, the threshold of the process. This would explain the constant value of μ, and therefore of τ_m and l, for a given sample to yield the straight lines observed in the experimental data. Actually, different temperatures will give a series of maxima, around M, slightly displaced from one another. This fact can explain, at least partially, the differences in threshold and slope of the lines (ln P versus $1/\bar{E}$) observed by delivering different energy densities to the irradiated sample.

Initially Free Electrons and the Effect of Laser Pulse Duration

In Ref. 14 the following expression was assumed for the breakdown probability given by an optical field:

$$P(\bar{E}) = N(\tau_L/\tau_{\text{coll}})f^{\text{M}} \exp(-\varepsilon_i/e\bar{E}l), \tag{6}$$

where N is the number of initially free electrons in the focal volume, τ_L is the duration of the laser pulse, f is the fraction of collisions that contribute to the process (i.e., lucky), and M is the number of half-cycles of the field required for the electron to reach ε_i. The dependence of $P(\bar{E})$ on N and τ_L is now considered.

For solids many processes have been invoked to explain the generation of the initially free electrons[4]: (i) the ionization of impurities, (ii) the ionization of shallow traps, and (iii) the direct ionization, by multiphoton absorption, of the molecule itself. Processes (i) and (ii) are considered the most likely in liquids also.

The role of impurities appears clearly from the experiments with tap water and with distilled water. In the latter case the breakdown threshold is higher (Fig. 4), probably because a lower concentration of impurities gives a lower concentration of electrons, which take part in the breakdown process. Furthermore, for N to be independent of $\bar{E}$, as indicated by the experimental results (Fig. 1), the process of initial electron generation must be easily saturated by the laser pulse. According to this interpretation, the breakdown threshold should be even higher in the highly purified HPLC water. Experimentally this is not so: the breakdown threshold is, in this case, even lower in comparison with tap water, as is shown in Fig. 2. This could be explained by the evolution of excess electrons in water. It has been experimentally shown[33] that excess electrons thermalize and reach, in 110 fsec, localized (prehydrated) states in preexisting trapping sites or molecular clusters. This transient species has a lifetime of ~240 fsec. Then solvation in deeper traps occurs, through configurational relaxation of the medium in the electron field. The fully relaxed electrons, in liquid water at room temperature, exhibit an optical absorption band with a peak at ~1.7 eV, which corresponds to the binding energy of the solvated state.[27] A steady-state situation is reached 2 psec after electron injection.[33] Within ~300 fsec after injection, the optical field at 1.06 μm can still make the electron free, through single-photon absorption, since the prehydrated state absorbs at this wavelength. After this time, when the solvated state is reached, creation of a free electron requires two photons at 1.06 μm.

The situation can be quite different in HPLC water. This medium, owing to its relatively ordered structure, can be more appropriately treated as a semiconductor[34] with an extended conduction band that has an edge at ~1.2 eV below the vacuum level.[27] A solvated electron can be raised to this band by an amount of energy of ~0.5 eV, i.e., in principle through a single-photon process. A deep trap in ordinary water would thus become a shallow trap in HPLC water. This fact, together with a more efficient Bragg reflection, can contribute to lower the breakdown threshold of this medium.

The direct ionization of the water molecules themselves, by multiphoton absorption, requires intense fields, which can be obtained with ultrashort laser pulses. Thus, experimentally, the effect can be studied together with that of the laser-pulse duration. Experimental results of ln P versus $1/\bar{E}$ in distilled water, obtained with pulses of different duration and with the same focusing optics, are shown in Fig. 3. An increase of the breakdown threshold and of the slope of the straight lines with shorter pulses is immediately evident. Equation (6) assumes that P depends linearly on τ_L simply because a longer pulse makes the required sequence of events more likely to occur. In the present case, this linear relationship is not verified. This is probably because, with intense laser fields, other factors in the expression of P such as the number N of initially free electrons depend on the field itself. This would certainly be the case if multiphoton ionization of the water molecule should occur. An estimate of the effectiveness of this process in the present conditions can be made[35] by considering the number of events per unit volume during the pulse duration and using the theoretical expressions for the ionization rate given by Keldysh[36] in the limit of high frequency. An evaluation for picosecond pulses[35] generated by a mode-locked Nd:YAG laser for the case of single molecules [Eq. (21) of Ref. 36], with ε_i = 12.6 eV, gives an electron density too low to initiate the breakdown process. However, a different result is obtained by using the theoretical expression [Eq. (41) of Ref. 36] that is valid for the creation of electron–hole pairs in semiconductors and ε_i = 6.5 eV, appropriate for liquid water.[27,28] In this case, in fact, with the threshold irradiance values obtained for the case of distilled water (Table 3), the density of electrons generated over a time duration of $\tau_L/10$ has the following order of magnitude: $N \sim 10^{11}$ cm^{-3} with 7-nsec pulses, $N \sim 10^{16}$ cm^{-3} with 220-psec pulses, and $N \sim 10^{17}$ cm^{-3} with 30-psec pulses. Since the value of N required for breakdown[4] is 10^{17}–10^{18} cm^{-3}, the occurrence of multiphoton ionization can be excluded for Q-switched nanosecond pulses, whereas it is in the range of contributing effects for 30-psec pulses. This can explain the difference in the experimental data represented, for these extreme cases, in Fig. 3. Here the higher slope of curve ln P versus $1/\bar{E}$, obtained with short pulses, could simply represent a thresholdlike behavior of the multiphoton ionization. The relevance of a molecular process independent of impurities

Table 3. Threshold Irradiance for Breakdown in Distilled Water with Laser Pulses of Different Durations

Pulse Duration (psec)	Spot Size (μm)	Threshold $\times 10^{10}$ (W/cm^2)
7000	75	3.45
7000	94	3.10
7000	230	1.37
7000	350	1.06
220	37	29.46
220	75	10.81
220	120	3.24
30	37	64.13
30	75	15.22
30	120	4.84

or traps is also evidenced by the fact that the threshold irradiance, with short pulses, is practically the same in tap water, distilled water, and saline solution (Fig. 4). On the other hand, the lower slope, obtained with nanosecond pulses, shows the common probabilistic character and should be due, as already discussed, mainly to ionization of impurities. The intermediate case, obtained with excitation by 220-psec pulses, shows an intermediate character: thresholdlike at lower fields (the same slope as with 30-psec pulses) and probabilistic at higher fields (the same slope as with 7-nsec pulses). The occurrence of these two regimes with this sequence has been considered explicitly in the literature.[4]

CONCLUSIONS

Experiments on laser-induced breakdown in water show that the physical mechanism responsible for this effect is, as in solids, electron avalanche ionization. An extended analysis of the experimental data allows many aspects of the process to be clarified.

Several theoretical models, developed for solids in a static field, predict for the breakdown probability P a dependence on the field as $\exp(-K/\bar{E})$ when the electrons avoid collisions in a ballistic flight and $\exp(-K'/\bar{E}^2)$ when the electrons undergo a lucky drift that avoids energy relaxation. K is proportional to the ionization energy ε_i; K' is proportional to ε_i and to the energy of photons that interact with the electrons. When breakdown is produced by an optical field, another effect must be present in the electron motion: the occurrence of lucky collisions, which reverse the electron momentum when the field reverses, so that the electrons can gain energy from the field. Bragg backscattering can be responsible for this effect. In fact, the value of the intermolecular distance in water, as deduced from scattering experiments, indicates that the electron wavelength, in the energy range of interest, satisfies the required Bragg condition.

The theoretical model, with the addition of the mechanism for lucky collisions, represents the experimental data well. The curves ($\ln P$ versus $1/\bar{E}$), in fact, present a linear part and a parabolic arc with a relative extension that depends on the degree of purity of the sample. Fitting the parabolic arc yields, as mentioned, a phonon energy. This energy can be evaluated well in the extreme cases of tap (i.e., impure) water and of HPLC (i.e., ultrapure) water. In the former case the frequency of an intermolecular (Raman) vibration is found; in the latter, the frequency of a collective dipolar motion.

The linear part of the experimental curves extends over a large field interval, thus showing stability against the small density variations of the medium during the initial transient. This behavior is explained well by the dependence of electron mobility on density in dense vapors.

An important role in the breakdown process is played by the electrons that initiate the avalanche. Ionization of impurities certainly provides most of these electrons in ordinary water. However, the ionization of shallow traps should also be important in ultrapure water. In this case, the presence of a conduction band in a semiconductorlike representation of the medium should make solvated electrons behave as shallow traps, thus possibly contributing to the process.

Finally, the direct ionization of water molecules by multiphoton absorption appears a likely process only with the intense fields of ultrashort pulses. In comparison with nanosecond excitation, the use of picosecond pulses produces a substantial increase in the breakdown threshold and in the slope of the ($\ln P$ versus $1/\bar{E}$) lines. Owing to electron generation through multiphoton ionization, the process seems more thresholdlike than probabilistic. The two regimes appear with the use of laser pulses of intermediate duration.

REFERENCES

1. C. De Michelis, "Laser induced gas breakdown: a bibliographical review," IEEE J. Quantum Electron. **QE-5,** 188–202 (1969).
2. Yu. P. Raizer, "Breakdown and heating of gases under the influence of a laser beam," Sov. Phys. Usp. **8,** 650–654 (1966) [Usp. Fiz. Nauk **87,** 29–36 (1965)].
3. A. J. Glass and A. H. Guenther, "Laser induced damage of optical elements—a status report," Appl. Opt. **12,** 637–649 (1973).
4. N. Bloembergen, "Laser-induced electric breakdown in solids," IEEE J. Quantum Electron. **QE-10,** 375–386 (1974).
5. P. A. Barnes and K. E. Rieckhoff, "Laser-induced underwater sparks," Appl. Phys. Lett. **13,** 282–284 (1968).
6. A. Vogel and W. Lauterborn, "Acoustic transient generation by laser-produced cavitation bubbles near solid boundaries," J. Acoust. Soc. Am. **84,** 719–731 (1988).
7. D. Aron-Rosa, J. J. Aron, J. Griesemann, and R. Thyzel, "Use of the neodymium:YAG laser to open the posterior capsule after lens implant surgery: a preliminary report," J. Am. Intraocul. Implant. Soc. **6,** 352–354 (1980).
8. F. Fankhauser, P. Roussel, J. Steffen, E. Van der Zypen, and A. Cherenkova," Clinical studies on the efficiency of high power laser radiation upon some structure of the anterior segment of the human eye: first experiments of the treatment of some pathological conditions of the anterior segment of the eye by means of a Q-switched laser system," Int. J. Ophthalmol. **3,** 129–139 (1981).
9. M. A. Mainster, D. H. Sliney, C. D. Belcher, and S. M. Buzney," Laser photodisruptors: damage mechanisms, instrument design and safety," Ophthalmologica **90,** 973–991 (1983).
10. S. P. Dretler, "Laser lithotripsy: a review of 20 years of research and clinical applications," Lasers Surg. Med. **8,** 341–356 (1988).
11. C. A. Puliafito and R. F. Steinert, "Short pulsed Nd:YAG laser microsurgery of the eye: biophysical considerations," IEEE J. Quantum Electron. **QE-20,** 1442–1448 (1984).
12. F. Docchio, L. Dossi, and C. A. Sacchi, "Q-switched Nd:YAG laser irradiation of the eye and related phenomena: an ex-

perimental study. I: Optical breakdown determination for liquids and membranes," Laser Life Sci. **1,** 87–103 (1986).
13. F. Docchio, C. A. Sacchi, and J. Marshall, "Experimental investigation of optical breakdown thresholds in ocular media under single pulse irradiation with different pulse durations," Lasers Ophthalmol. **1,** 83–93 (1986).
14. M. Bass and H. H. Barrett, "Avalanche breakdown and the probabilistic nature of laser-induced damage," IEEE J. Quantum Electron. **QE-8,** 338–343 (1972).
15. W. Shockley, "Problems related to P-N junctions in silicon," Czech. J. Phys. B **11,** 81–86 (1961); Solid-State Electron. **2,** 35–40 (1961).
16. E. Yablonovitch, "Optical dielectric strength of alkali-halide crystals obtained by laser-induced breakdown," Appl. Phys. Lett. **19,** 495–497 (1971).
17. M. Zahn, Y. Ohki, D. B. Fenneman, R. J. Grisphover, and V. H. Gehman, Jr., "Dielectric properties of water and water/ethylene glycol mixtures for use in pulsed power system design," Proc. IEEE **74,** 1182–1220 (1986).
18. P. A. Wolff, "Theory of electron multiplication in silicon and germanium," Phys. Rev. **95,** 1415–1420 (1954).
19. G. A. Baraff, "Distribution functions and ionization rates for hot electrons in semiconductors," Phys. Rev. **128,** 2507–2517 (1962).
20. L. V. Keldysh, "Concerning the theory of impact ionization in semiconductors," Sov. Phys. JETP **21,** 1135–1144 (1965).
21. B. K. Ridley "Lucky-drift mechanism for impact ionisation in semiconductors," J. Phys. C **16,** 3373–3388 (1983).
22. F. Seitz, "On the theory of electron multiplication in crystals," Phys. Rev. **76,** 1376–1393 (1949).
23. B. N. Brockhouse, "Structure dynamics of water by neutron spectrometry," Nuovo Cimento Suppl. **IX,** 47–75 (1958).
24. A. H. Narten and H. A. Levy, "Liquid water: molecular correlation functions from x-ray diffraction," J. Chem. Phys. **55,** 2263–2269 (1971).
25. E. Kálmán, G. Pálinkás, and P. Kovács, "Liquid water. I: Electron scattering," Mol. Phys. **34,** 505–524 (1977).
26. G. Pálinkás, E. Kálmán, and P. Kovács, "Liquid water. II: Experimental atom pair-correlation functions of liquid D_2O," Mol. Phys. **34,** 525–537 (1977).
27. D. Grand, A. Bernas, and E. Amouyal, "Photoionization of aqueous indole; conduction band edge and energy gap in liquid water," Chem. Phys. **44,** 73–79 (1979).
28. J. W. Boyle, J. A. Ghormley, C. J. Hochanadel, and J. F. Riley, "Production of hydrated electrons by flash photolysis of liquid water with light in the first continuum," J. Phys. Chem. **73,** 2886–2890 (1969).
29. Z. Cardeny and J. Tauc, "Hot-carrier thermalization in amorphous silicon," Phys. Rev. Lett. **46,** 1223–1226 (1981).
30. G. Ascarelli, "Experimental detection of collective modes in a polar liquid: application to the case of the solvated electron in H_2O and NH_3," Can. J. Chem. **55,** 1916–1919 (1977).
31. J. G. Fujimoto, W. Z. Lin, E. P. Ippen, C. A. Puliafito, and R. F. Steinert, "Time-resolved studies of Nd:YAG laser-induced breakdown: plasma formation, acoustic wave generation, and cavitation," Invest. Ophthalmol. Vis. Sci. **26,** 1771–1777 (1985).
32. P. Krebs, "Localization of excess electrons in dense polar vapors," J. Phys. Chem. **88,** 3702–3709 (1984).
33. A. Migus, Y. Gauduel, J. L. Martin, and A. Antonetti, "Excess electrons in liquid water: first evidence of a prehydrated state with femtosecond lifetime," Phys. Rev. Lett. **58,** 1559–1562 (1987).
34. F. Williams, S. P. Varma, and S. Hillenius, "Liquid water as a lone-pair amorphous semiconductor," J. Chem. Phys. **64,** 1549–1554 (1976).
35. A. Penzkofer, "Parametrically generated spectra and optical breakdown in H_2O and NaCl," Opt. Commun. **11,** 265–269 (1974).
36. L. V. Keldysh, "Ionization in the field of a strong electromagnetic wave," Sov. Phys. JETP **20,** 1307–1314 (1965) [Zh. Eksp. Teor. Fiz. **47,** 1945–1957 (1964)].